

# Intelligent Prediction and Data Service Ptimization Scheme of Power Grid Based on Improved Bee Colony Algorithm

Bo Liu

China Southern Power Grid Digital Platform Technology Company  
Guangzhou, Guangdong, 510000, China  
liubo6@csg.cn

Wang Zhou

School of Science of Zhejiang Sci-Tech University  
Hangzhou, Zhejiang, 310018, China  
zhouwang@csg.cn

Haowen Ren

School of Electrical Engineering Northeast Electric Power University  
169 Changchun Road, Jilin, 132012, China  
renhw@csg.cn

Zhongkai Fan

School of Electrical Engineering Northeast Electric Power University  
169 Changchun Road, Jilin, 132012, China  
fanzk@csg.cn

\*Corresponding author: Bo Liu

Received February 27, 2023, revised May 7, 2023, accepted August 9, 2023.

---

**ABSTRACT.** *In recent years, the power industry is facing more and more new cyber threats, with the Ukrainian power grid being attacked twice, triggering large-scale black-outs, and the Iranian nuclear power being attacked by virus voltage. Therefore, realizing intelligent prediction and data service optimization of complex power grid has remarkable positive significance. In this paper, we combine narrow-band filter detection method, adaptive learning algorithm and piecewise linear regression analysis technique to build the model of power grids. Then according to the characteristic parameters of the grid, combining with the link prediction algorithm and the optimized Dijkstra algorithm, an optimization method of the grid characteristic model is proposed considering outliers of the reconstructed network, so as to better provide instructive suggestions for the overall network restoration. Then, this paper analyzes some algorithms, such as the classical link prediction algorithm, the anomalous edge link prediction algorithm and anomaly-based grid intelligent prediction algorithm. Not only the multi-objective swarm optimization algorithm but the anomalous link prediction swarm intelligent optimization algorithm is proposed to solve the grid model in this article. By using the SIOA-ALP anomaly link prediction swarm intelligent optimization algorithm and other benchmark social network opinion propagation control methods, the simulation experiment of topological power grid anomaly link prediction is realized. Comparing the experimental results under different data sets, and supplemented with the statistical checkout, advantages of the model and algorithm given in the paper are fully reflected, which can provide a better intelligent prediction and data service optimization scheme for complex large-scale power grid. At the end of this paper, the relevant research directions in the future are prospected and predicted.*

**Keywords:** bee colony algorithm; power grid intelligent prediction; data service; improved Dijkstra algorithm; link prediction

**1. Introduction.** Traditional security products, such as firewalls, IPS, vulnerability scan, etc., perform attack identification and protection based on signed certificates and static rules [1, 2]. Digital grid is a new energy ecosystem formed by the core driving force of new generation digital techniques. Data becomes a significant production factor, modern electric energy network and advanced information network become the foundation, continuously improving the extent of digital intelligent network construction through the deep integration of digital technology with operation and management of energy corporations. Flexibility, openness, interactivity, economy and sharing are the characteristics, making the grid more intelligent, safe, reliable, green, and efficient [3, 4]. The digital power grid is similar to the digital twin manufacturing, which is essentially a continuous optimization system of the whole life cycle of the complex virtual reality integrated grid. The digital grid is also based on a unified digital grid model, which enables the collection and analysis of various data from the physical power grid through connection channels such as the data network/Internet of things and the like, and interacts with people through applications such as grid management platforms, thus realizing entire life cycle optimizations, such as projecting, design, and construction until finishing the operation [5, 6].

Some scholars have considered the voltage regulation of distribution grid to solve the overvoltage problem, but this method may increase the grid pressure through excessive operation and high loss of grid equipment [7, 8, 9]. On the basis of grid voltage analysis, Xie et al. [10] used the intelligence information from security manufacturers to correlate the characteristics and influence scope of the grid threat, to concentrate the superior resources to take treatment measures to deal with those critical grid threats in a timely manner, and to carry out early warning for the grid voltage events with higher accuracy and threat level, to realize automatic strategy linkage, and further improve the efficiency of emergency response treatment. Therefore, in order to make grid voltage obtain overall

improvement, many different optimization objectives are able to be taken into consideration and the problem can be regarded as the best voltage regulation issue [11]. Optimal regulation schemes based on optimization methods have been proposed to solve distribution networks, where most of the reactive power capabilities are combined with network structures, including disconnecting switches and other regulators to optimize the grid voltage. Srivastava et al. [12] proposed to redistribute reactive power with grid units to minimize grid voltage loss.

In addition, some scholars have established several optimization objectives with the aim of minimizing grid power [13, 14, 15]. To seek better efficiency and accuracy which belong to the power grid voltage optimization, existing grid optimization methods usually contain multiple objectives, so the above problem can be transformed into a simplified two-objective optimal voltage regulation issue. Gao [16] considers that the classical optimal grid regulation scheme has the problem of high time complexity, and carries out grid voltage optimization based on quasi-linear real-time optimal algorithm. Other scholars used dynamic detection technologies. For instance, using deep learning and machine learning to construct the framework of grid voltage threat detection technology [17, 18], while Sheng et al. [19] developed a layering electrical control system for grid parallel coordination. Some scholars have proposed a meta-heuristic technique obtain the optimal solution of voltage regulation issue. For example, some scholars used fuzzy differential evolutionary algorithm to solve the above problem [20, 21], and some scholars have also analyzed the influence of parameters such as the strength of grid topological coupling on grid stability [22, 23, 24, 25]. In this study, subspace reconstruction and availability analysis is adopted to construct the complex network model of the grid, and a prediction algorithm is designed for the grid link network. Then the method is improved by combining the anomaly value and the improved Dijkstra algorithm, and get the solution of the model with the improved bee colony algorithm. That is getting more useful data service when facing the complex multi-network center environment of the grid, to realize the automatic construction, rapid scheduling, intelligent dispatching and joint utilization and version release management among service interfaces for large-scale heterogeneous services of digital power grid, and ensure high availability and high concurrency of the grid service. It can greatly raise physical resource utilization, save hardware cost, development cost, operation and maintenance cost, and improve service release efficiency. The following sentences describe other parts of this article. The second part summarizes the theoretical framework; the third part parents the design framework which describes the algorithm; in the fourth part, the experimental results would be given; finally, the conclusions and prospectives are given in the fifth part.

## 2. Model construction.

**2.1. Construction of the grid model.** In this study, a complex network approach is used to implement modeling of the power grid, with reference to the literature [26, 27, 28], using a graph  $G = (V, E)$  to present the grid model, assuming that the edge vector of the circuit node data distribution is  $(u, v) \in E$ . At the terminal of electronic circuit information transmission, a narrowband filter detection method is used for adaptive detection of electronic circuit nodes, combined with a matched filter detector for adaptive filtering, an adaptive learning algorithm is used for distributed feature reconstruction of electronic circuit nodes, segmented linear regression analysis technique can be used to build a statistical analysis model containing data of electronic circuit nodes. We set the reference variable of circuit fault sampling as  $x'(t)$  and the template variable as  $s'(t)$  under the big data fusion mode, and adopt the group detection method to obtain the parameter

estimates, which is shown in Equation (1).

$$\begin{cases} x'(t) = x(t) * h_w(t) \\ s'(t) = s(t) * h_w(t) \end{cases} \quad 0 \leq t \leq T \quad (1)$$

The load information flow of the electronic circuit fault point is extracted, and an envelope contour detection method is adopted to for sampling and adaptive modulation of the electronic circuit fault point to obtain the modulated variable output, as shown in Equation (2).

$$d(t) = a_0 (x'(t) + s'(t)) \quad (2)$$

In addition, set  $S_0(t) = a_0\delta(t)$ , which indicates the existence of the finite set of vectors in the connected graph of the electronic circuit fault point distribution. Then we use the adaptive feature estimation of the electronic circuit fault point to obtain the output signal feature quantity,  $S(t)$ , and the multipath delay characteristic distribution is shown in Equation (3).

$$S(t) = a_0 \sum_{i=1}^N a_i \delta(t - \tau_i) e^{j\omega t} \quad (3)$$

The wide time domain window  $S_r(t)$  for constructing the characteristic distribution of fault points in electronic circuits is shown in Equation (4).

$$S_r(t) = S(t) * h(t) + n_s(t) \quad (4)$$

Where,  $n_s(t)$  is the spectral noise on the time axis. Then we construct the statistical sequence distribution model of electronic circuit fault points, and use the big data mining method for the collection of electronic circuit fault point information, which is tenable when Equation (5) is satisfied.

$$\begin{cases} 1, \text{sgn}(|z(k)|^2 - R_{MDMMA}(k)) = \text{sgn}(|z(k)|^2 - R) \\ 0, \text{sgn}(|z(k)|^2 - R_{MDMMA}(k)) \neq \text{sgn}(|z(k)|^2 - R) \end{cases} \quad (5)$$

According to the references [29, 30], apply doppler suppression to  $p(-t)$ , use correlation spectrum feature detection method for the acquisition of electronic circuit fault point anomaly data, match the filtering of the collected electronic circuit fault point information feature quantities, and sample the features of fault point data to construct a fault distribution data set based on the filtering detection results. In addition, our research considers the grid mixed integer nonlinear optimization problem under the isolated switch. We set the isolated regulator position as a discrete control variable, and the Pareto front solution which belongs to this Binocular optimization issue can be obtained. Then,  $X(i, j)$  and  $Y(i, j)$  can be shown as the coefficients calculated by Equation (6–7), while the grid power flow can be expressed by Equation (8).

$$f(w_1, w_2) = w_1 * \sum_{\Delta t} (t - \Delta t) + w_2 * \Delta C(t) \quad (6)$$

$$\{X(i, j), Y(i, j)\} = [R(i, j)/(V(t, i) * V(t, j))] * \{\cos(i, j), \sin(i, j)\} * \Delta t \quad (7)$$

$$\{O(t, i), L(t, i)\} = V(t, i) * \Delta t * \left\{ \sum_{i, j} V(t, j) * \{X(i, j), Y(i, j)\}, \sum_{i, j} V(t, j) * \{X(i, j), Y(i, j)\} \right\} \quad (8)$$

In addition, the voltage magnitude  $V(t, s)$  can be constructed from the grid voltage magnitude  $V(t, h)$  shown in Equation (9) for the isolation switch, which indirectly makes the distribution network in a limited situation of the voltage stability. And as shown in the literature [12], the grid voltage deviation has a strong dependence on the network stability. Finally, the reactive power capability and the operating range of the disconnect

switches are introduced, in which  $Q(t, n)$  and  $Q(t, x)$  are some corresponding limit values, which can be obtained by Equation (10).

$$V(t, s) = V(t, h) / \left[ \prod (e^{f(\alpha+\beta)})^2 / \sum e^{f(\alpha+\beta)} \right] \quad (9)$$

$$\{L(t, n), L(t, x)\} = \pm \sqrt{(S(i) + O(t, d)) * (S(i) - O(t, d))} \quad (10)$$

where  $S(i)$  describes the rated power which belongs to the grid at the  $i^{\text{th}}$  panel point. The computational compicacy of the classical optimization issue has a close relationship with the grid topology, hence this optimal operation which belongs to the grid cannot be guaranteed. In contrast, the distribution system determines the time frame of the planning stage, using the selected disconnect switches with update rules as inputs for reactive power allocation.

**2.2. Model Optimization Based on the Grid Characteristic Parameters.** The goal of the grid prediction and governance is that in the state of large-scale network failure, the powered generating units can be supplied with the shortest path to the candidate restoring units prioritized by their anomaly degree, thus rebuilding the system grid and accelerating the system recovery process. After that, the link anomaly degree is used as a criterion to sequentially restore the candidate restoring lines around the recovered ones [31, 32, 33]. Therefore, the link prediction method in complex networks can be applied as a reconfiguration indicator for screening important nodes and critical lines to provide guidance for determining the reconfigured network. The substance for applying link prediction algorithms and reconfiguring this power system skeleton network is to calculate the restoration sequence of actual generator power nodes and achieve power supply to all lost units in the network by some link prediction method after a large-scale power outage, and to lay the foundation for the restoration in the next path [34, 35, 36, 37]. In this study, this link prediction algorithm which owns strong prediction precision can be used to obtain the ranking score  $RS_e$  of each edge  $e$ , i.e., the anomaly degree, and then calculate the anomaly degree  $RS_x$  of all power nodes to be restored and prioritize the power nodes with higher anomaly degree in the restoration graph. After determining the recovery order of power nodes, the shortest path from the power node to be recovered to other charged power nodes is calculated using the improved Dijkstra algorithm (as shown in Algorithm 1) [38], from which the connected power node skeleton graph can be obtained; after the skeleton network reconstruction is completed, the paths around the generator power supply are recovered in order from the highest to the lowest by the anomaly degree of the edges, so as to achieve the recovery of the whole network.

Since the reconfiguration process involves many technical factors as well as uncertainties, the network reconfiguration guidance is performed with the help of the network construction which ensures to satisfy the operational quality [39, 40, 41]. Considering the importance of anomalous edges and anomalous panel points to the meshwork, if the number of anomalous edges and anomalous panel points contained in the reconstructed network become bigger, the reconfiguration method would be more effective, so this paper defines the reconstructed network efficiency  $\eta = \bar{r}/\bar{c}$ , where the larger  $\eta$  is, the higher the reconfiguration efficiency would be,  $\bar{r}$  denotes the average anomaly of comprehensive load panel points which come from the reconstructed meshwork, and  $\bar{c}$  denotes the clustering

---

**Algorithm 1** Application of Improved Dijkstra Algorithm in Power Grid
 

---

**Input:**  $G = (V, E)$ ,  $x \in V$ ,  $e \in E$ 
**Output:** path  $(i - 1, i)$ 

```

1: for  $i, j = 1: k$  do           // Sorted power node labels
2:   path  $(i, j) = \text{dijkstra}(A, i, j)$    // Shortest path calculation using improved
   Dijkstra's algorithm
3:   if path  $(i - 1, i) \leq \text{path}(j, i)$  ( $i \geq 2, 1 \leq j \leq i - 1$ ) then   // Ensure the
   priority and rapid recovery of critical nodes
4:     else
5:       path  $i = \text{path}(i - 1, i)$        // Obtain the reconfigured skeleton network
   composed of power nodes
6:     end if
7: end for

```

---

coefficient of this reconstructed network as shown in Equation (11).

$$\left\{ \begin{array}{l} \bar{r} = \frac{\sum_{i=1}^k \frac{r_i}{\max(r_1 r_2 \cdots r_k)}}{k} \\ \bar{c} = \frac{\sum_{j=1}^m \frac{c_j}{\max(c_1 c_2 \cdots c_m)}}{m} \\ c_j = \frac{2d'_j}{d_j(d_j - 1)} \end{array} \right. \quad (11)$$

where  $k$  describes the quantity of load panel points contained from the reconfigured network,  $m$  describes the quantity of panel points from the reconfigured meshwork,  $d_j$  describes the degree of panel point  $j$  when facing the original network, and  $d'_j$  is the degree of panel point  $j$  when facing the reconfigured network. Moreover, when actually operating the grid, the receiving terminal which belongs to this grid tends to increase the purchase of external power when the load is high, otherwise the opposite conclusion. So that this external power follows the load trend to a certain extent, and has a certain peaking effect, so the peaking capacity of the external power should be taken into account. According to the previous topic, the peaking factor can take the peaking capacity of the EHV district electricity into account as long as it has been given. Referring to the definition of the peaking rate of conventional generating units, the peaking rate of external power in the zone during the cycle can be determined by Equation (12).

$$k_{\text{line}} = \frac{P_{\text{line, max}}(t) - P_{\text{line, min}}(t)}{P_{\text{line, max}}(t)} \quad (12)$$

where,  $P_{\text{line, max}}(t)$  represents the maximum value of regional external power output in the period, and  $P_{\text{line, min}}(t)$  represents the minimum value. In order to achieve the efficient reconfiguration strategy, it is necessary to connect all power nodes and load nodes with relatively few lines to form a skeleton network, so as to better guide the recovery process of the whole network. The specific algorithm can be seen in Algorithm 2.

### 3. Algorithm optimization.

**3.1. Classical Link Prediction Algorithm.** Based on the power grid optimization model mentioned above, the grid can be abstractly transformed into a graph which contains a node set and an edge set. In the process of recording the meshwork, due to the

**Algorithm 2** optimization method of power grid feature model**Input:**  $G = (V, E)$ ,  $x \in V$ ,  $e \in E$ **Output:**  $\{RS_x\}$ 

- 1: **for**  $i = 1 : 5$  **do**
- 2:     Calculate  $RS_i$
- 3: **end for**
- 4: Let  $LPA = LPA_i$  s.t.  $RS_i = \min \{RS\}$      // Select the link prediction algorithm (LPA) with the highest prediction accuracy
- 5: Let  $RS_e = LPA[train, e]$      // Calculate the anomaly of each edge
- 6: Calculate  $RS_x$  and sort (descend)  $\{RS_x\}$      // Obtain the sorted power nodes and determine the priority recovery order of the power nodes
- 7: Return the best solution (binary vector)

incompleteness of information, there observes link loss problems in the network, such as information loss and deliberate information hiding. The actual work of network link prediction can be used to predict the degree of whether there exists one connection during double panel points which is located in a meshwork where a connected edge has not been produced. This prediction includes predictions of both unknown links and future links. Link prediction relates networks to information science and deals with the restoration and prediction of missing information in information science. Scholars have used the proximity during panel points, i.e. the likelihood for a link which is located in double panel points, directly for link prediction. The typical similarity index based on local structure information includes CN [42] , AA [43] , PA [44] and RA [45] , and path-based typical similarity index includes LP [46] , ERA [47] , PIC [48] and so on. The main indicators to survey the precision for the link prediction algorithm include AUC [49], precision [50] and Ranking score [51], among which AUC can be used as the most normal measurement, which can describe the accuracy of the algorithm as a whole, while the ranking score takes into account the ranking of the predicted edges. The specific definition methods of the above similarity metrics are as follows.

In the well-known structural local metric method,  $CN(u, v)$  represents common neighbor nodes shared between double panel points  $u$  and  $v$  amid a social meshwork and the number of which would be given. And let  $\tau(u)$  shows the set of neighbors of panel point  $u$ . That normal neighbor mensuration will be defined and the content is expressed in Equation (13).

$$CN_{uv} = |\tau(u) \cap \tau(v)| \quad (13)$$

The Adamic/Adar score is shown in Equation (14). Preferential attachment [31] can be expressed by PA. It is presumed that the degree of whether a new link can be connected to panel point  $u$  changes in the same trend with  $|\tau(u)|$ , so the preferential attachment of panel points  $u$  and  $v$  change in the same trend with the quantity of their adjacent objects, which can be calculated by Equation (15).

$$AA_{uv} = \frac{1}{\log |\tau(x)|} + \frac{1}{\log |\tau(y)|} + \frac{1}{\log |\tau(z)|} + \frac{1}{\log |\tau(t)|} = 4.51 \quad (14)$$

$$PA_{uv} = |\tau(u)| \cdot |\tau(v)| \quad (15)$$

RA can represent Aesource Allocation, which is calculated upon the transversion of allocating meshwork resources, where the normal neighbors of double detached panel points  $u$  and  $v$  are thought as the objects who send resources, in which each panel point provides a unit that enables node  $u$  to send some resources to  $v$ , as shown in Equation

(16).

$$RA(u, v) = \sum_{z \in (\tau(u) \cap \tau(v))} \frac{1}{|\tau(z)|} \quad (16)$$

Local Path index (LP). Local path index method offers a nice compromise when handling the precision and computational sophistication of local link prediction techniques and global link prediction techniques, which is a local link prediction method. If  $x$  and  $y$  are irrelevant,  $(A^3)_{xy}$  describes various paths with the length of 3 which are in the middle of  $x$  and  $y$ . The key is also likely to extend to a generalized form as shown in Equation (17).

$$S^{LP} = A^2 + \varepsilon A^3 + \varepsilon^2 A^4 + \dots + \varepsilon^{(n-2)} A^n \quad (17)$$

where  $n$  is the maximum number of orders. Extended Resource Allocation (ERA) is an extended resource allocation metric, and is proposed for a potential resource transmitted between two nodes through a local path, based on the exchange of resources between nodes. This can be shown by Equation (18). Potential Information Capacity (PIC) is to define information content, which is thought as to describe the scale of information transmission content between any double panel points according to Canny's law, taking information channel and information context into consideration. This can be shown by Equation (19).

$$S_{xy}^{ERA} = \sum_{z \in C_{xy}} \frac{2 + \sigma * (n_{zy} + n_{zx})}{k_z} + \sum_{C'_{xy}} \frac{\sigma * (n_{zy} + n_{zx})}{k_z} \quad (18)$$

$$S_{xy}^{PIC} = \sum_{z_y \in \Gamma(y)} \left( a_{xz_y} + \frac{n_{xz_y}}{k_{z_y}^{\max} - 1} \right)^\beta + \sum_{z_x \in \Gamma(x)} \left( a_{yz_x} + \frac{n_{yz_x}}{k_{z_x}^{\max} - 1} \right)^\beta \quad (19)$$

**3.2. Anomalous Edge Link Prediction Algorithm.** For node pairs not yet connected in a network, the link prediction algorithm (similarity metric) owns the ability to predict the possibility whether an edge exists during double panel points. For those where a link already exists in the network, if the similarity algorithm obtains the value of similarity of this edge is very low, then their existence is of great significance to the meshwork. Referring to [52, 53], link prediction algorithms can be used to evaluate the reliability or importance of the existence of a link.

Anomalous edges are those real in the network but considered to have a low probability of existence by link prediction methods. Anomalous links have a particularly important contribution to maintain the connectivity of the network, and the anomalous link analysis method can effectively identify edges that play an important role in network connectivity. Therefore, it can be believed that prioritizing the recovery of anomalous edges in the network is an important guide for the recovery process of the network. For a given network  $G = (V, E)$  and a link prediction algorithm, the network data set is partitioned by a term-by-term traversal method: traversing each edge in the network to constitute the test set. For  $\forall e \in E$ , the algorithm yields the ranking of the edge's similarity  $s_e$  in the set of unknown edges  $H$ , denoted as  $r_e$ , and the ranking score which belongs to the edge  $e$  will be defined. Meanwhile, the concrete content is described as Equation (20).

$$RS_e = \frac{r_e}{1 + \frac{n(n-1)}{2} - |E|} \quad (20)$$

where  $|H| = 1 + \frac{n(n-1)}{2} - |E|$  denotes the set which contain every unknown edge, i.e., concatenating the test set and the set of nonexistent edges. For anomalous edges, a larger ranking score  $RS_e$  indicates a more anomalous level, so its anomalousness can be



expressed by its ranking score. For network  $G$ , traversing all the edges in which belong to the test set, the ranking score for the system can be obtained as shown in Equation (21).

$$RS = \frac{1}{|E^p|} \sum_{e \in E^p} RS_e = \frac{1}{|E^p|} \sum_{e \in E^p} \frac{r_e}{|H|} \quad (21)$$

For a node  $x$ , the ordering score of the system  $G_0(V_x, E_x)$  constructed by its associated edges and itself can be expressed as shown in Equation (22).

$$RS = \frac{1}{|E_x^p|} \sum_{e \in E_x^p} RS_e = \frac{1}{d_x} \sum_{e \in E_x^p} \frac{r_e}{|H|} \quad (22)$$

Moreover, the definition of the anomaly degree of panel point  $x$  is as shown in Equation (23).

$$RS_x = \frac{1}{d_x} \sum_{z \in \Gamma(x)} \frac{r_{(x,z)}}{|H|} \quad (23)$$

In which,  $d$  describes the degree which belongs to the panel point,  $\Gamma$  describes the set of adjacency objects of the panel point,  $(x, z)$  denotes the edges connecting nodes  $x$  and  $z$ . And for the link prediction algorithm, the smaller the system ranking score indicates the better prediction of the algorithm; while for anomalous edges, the larger the ranking score indicates the more anomalous level of the links.

**3.3. Intelligent forecasting algorithm of power grid according to anomalous degree.** What is desired to get for grid prediction is to supply the powered generating units with the shortest path to the candidate restoring units in the state of massive network failure by prioritizing them according to their anomalous degree, so as to rebuild the system grid and accelerate the system recovery process; then the link anomalous degree is used as a criterion to sequentially restore the candidate restoring lines around those restored ones. Since power grids have certain commonalities of complex networks, link prediction methods in complex networks can be applied as reconfiguration indicators for screening important nodes and critical lines, providing guidance for determining reconfiguration networks. Applying link prediction algorithms tells the substance to reconfigure the skeleton network of power systems is to calculate the restoration sequence of actual generator power nodes, and realize the power supply of all lost units in the network by some link prediction method after a large-scale power outage to lay the foundation for the next path restoration [54, 55, 56]. Therefore, the link prediction algorithm which owns great prediction precision is used to obtain the ranking score  $RS_e$  for each edge  $e$ , i.e., the anomaly degree, and then calculate the anomaly degree  $RS_x$  for all the candidate restoring power nodes, and prioritize the power nodes with higher anomaly degree in the restoration graph. After determining the restoration order of power nodes, the shortest path from the candidate restoring power nodes to other power nodes is calculated using the improved Dijkstra algorithm, from which the connected power node skeleton graph can be obtained. After the grid structure reset is completed, the paths around the generator power would be restored in order from the highest to the lowest according to the anomaly degree of the edges, thus realizing the restoration of the whole network.

Since the prediction process involves many technical factors as well as uncertainty factors, the reconstruction of the meshwork is guided according to the meshwork structure which ensures to satisfy the operation quality [57, 58]. Considering the importance of anomalous edges and anomalous panel points to the meshwork, if the quantity according to anomalous edges and panel points contained in the reconstructed meshwork become

bigger, the reconstructed method would be more effective, so this paper defines the reconstructed network efficiency  $\eta = \bar{r}/\bar{c}$ . And the larger  $\eta$  is, the higher the reconstructed efficiency would be, and  $\bar{r}$  denotes the average anomaly of all load panel points in the reconstructed meshwork,  $\bar{c}$  denotes the clustering coefficient of the reconstructed network, which can be expressed in Equation (24) and Equation (25).

$$\bar{r} = \frac{\sum_{i=1}^k \frac{r_i}{\max(r_1 r_2 \cdots r_k)}}{k} \quad (24)$$

$$\bar{c} = \frac{\sum_{j=1}^m \frac{\frac{2d'_j}{d_j(d_j-1)}}{\max\left(\frac{2d'_j}{d_m(d_m-1)}\right)}}{m} \quad (25)$$

Where  $k$  shows the quantity of load nodes contained in the reconstructed meshwork,  $m$  is the quantity of panel points there,  $d_j$  is the degree of panel point  $j$  in the initial meshwork, and  $d'_j$  is that of panel point  $j$  in the reconstructed network. To achieve an efficient prediction strategy, it is necessary to link all power nodes and load nodes with high anomaly degree, to form a skeleton network with relatively few lines, which in turn can better guide the recovery process of the whole network.

### 3.4. Power grid optimization method based on improved bee colony algorithm.

Artificial Bee Colony (ABC) algorithm [59, 60], which can be thought as a meta-heuristic algorithm for mixed and numerical optimization issues. The process of finding food for bees gives it inspiration. Meanwhile, bees and food sources are double main components for ABC. Solutions to the issue are food, and bees can be seen as a factor in finding the best food source.

First and foremost, reference [61] searches the issue space. Then a random or specific strategy can be used to obtain a set of food sources. Those bees can be separated into three parts: worker bees, bystander bees and scout bees. Every initial food source  $S_i$  is a worker bee firstly, hence the quantity of initial food sources can be the quantity of worker bees. After that, the corresponding food source would be found in a neighboring node, and if the fresh food source owns more nectar than which the food source  $S_i$  owns, then the new food source will become the next place for the bees to move, and otherwise, they will keep in the same place. After the process, worker bees will choose to go back to their home and tell the bystander bees about relative food sources and their nectar amounts. Every bystander bee will select a food source randomly according to those information. The same as the worker bees, bystander bees can search to get solutions near the chosen food source by neighborhood arithmetic. If there exists more nectar which is available, that location will be their next new position, otherwise, they will choose to come back to the chosen food source. For the artificial bee colony algorithm, the quantity of bystander bees can be thought the same as that of worker bees. Then, the process can be iterative and the algorithm would search for the optimal solution to the problem.

Our study presents a swarm optimization approach for grid problems to set a set of panel points as solutions to make the spread of influence achieve the largest scale. For this purpose, the set of influences is identified in iterations and a different solution can be determined for every iteration. Then, the non-dominated solutions will arrange in order for the algorithm. Then, the optimal solution will be selected as the answer to this issue at the end. Every solution  $S_i$  is considered as a set of panel points  $S_i = \{s_{i,1}, s_{i,2}, s_{i,3}, \dots\}$ . Let the quantity of panel points be  $k$ , while the number of nodes in the multi-objective

bee colony algorithm varies depending on the required budget and spend for the panel points. Algorithm 1 gives a specific explanation of this algorithm. Algorithm 3 consists of four steps: initialization, worker bee, bystander bee and scout bee, where the initial food source (solution) is determined randomly in the initialization step.

---

**Algorithm 3** Solving process of multi-objective bee colony algorithm

---

**Input:**  $G(V, E, W)$ ,  $k$ ,  $FN$ ,  $\max_{Iteration}$ ,  $ch$ ,  $\beta$ ,  $EA\_size$

**Output:** initial seed set  $S$

```

1:  $S_h \leftarrow \text{highest\_weight\_degree}(G, k)$ 
2: for  $i = 2$  to  $FN$  do
3:    $S_i \leftarrow \text{neighborhood\_solution}(G, S_h, \beta)$ 
4:   Evaluate the nectar amount of food source  $S_i$ 
5: end for
6: while iteration < max iteration do
7:   for  $i = 1$  to  $FN$  do // worker bee
8:      $ns \leftarrow \text{neighborhood\_solution}(G, S_i, \beta)$ 
9:   end for
10:  Update non-dominant set in  $EA$ 
11:  for  $r = 1$  to  $FN$  do // bystander bee
12:     $ns \leftarrow \text{neighborhood\_solution}(G, S_r, \beta)$ 
13:  end for
14:  for  $i = 1$  to  $FN$  do // scout bee
15:    if  $ch_i = 0$  then
16:       $S_i \leftarrow \text{crossover\_solution}(EA, k)$ 
17:    end if
18:  end for
19:  Iteration  $\leftarrow$  Iteration + 1
20: end while

```

---

For worker bees, each node uses the neighborhood solution function to find a solution  $ns$  near its corresponding food source, if  $ns$  decide the current solution  $S_i$ , then the solution  $ns$  replaces  $S_i$  and the bee will choose to move to the food source  $ns$ . In addition, providing that the quantity of non-dominated solutions outstrips the scale of the EA, the algorithm which is about crowding distance can be used to determine and eliminate crowded solutions. Therefore, solution  $ns$  can take place of  $S_i$  inside the inner archive. and for the bystander bees, every bystander bee chooses a food source  $S_i$  randomly in the non-dominated set within the EA. Then, the degree of whether choosing food source  $S_i$  can be shown in Equation (26).

$$p_t = \frac{Cd_t}{\sum_{j=1}^{EA\_member} Cd_j} \quad (26)$$

where  $Cd_t$  describes the congestion distance value which belongs to solution  $S_t$ , and  $EA\_member$  describes the quantity of members in the external archive. Then the bee ensures an answer  $ns$  in its neighborhood, and if  $ns$  influences  $S_r$ , then the solution  $S_r$  will be substituted by  $ns$  in the EA. If both  $S_r$  and  $ns$  are neither dominant, then  $ns$  will be joined into EA as a non-dominated parts, and the non-dominated set would be updated at the end. And for scout bees, while the worker bees having no chance to search for their neighbors at their current position facing consecutive iterations before they turn into scout bees. Next, for every scout bee by the cross-solution function, a new food source will be generated, and that bee will be transported to the new source as a worker bee.

Firstly, this function chooses double non-dominated solutions randomly in the EA. Then, it merges them from a random overlap to generate a new solution [62, 63, 64, 65, 66, 67]. The Swarm Intelligent Optimization Algorithm for Abnormal Link Prediction (SIOA-ALP), that selects the optimal solution according to that non-dominated set (called Pareto boundary) in the inner of EA as the seed set optimization solution, can be represented as Algorithm 4 shown.

---

**Algorithm 4** Anomaly link prediction swarm intelligent optimization algorithm

---

**Input:**  $G = (V, E)$ ,  $x \in V$ ,  $e \in E$ ,  $EA$ ,  $k$ ,  $FN$ ,  $\max_{Iteration}$ ,  $ch$ ,  $\beta$ ,  $EA\_size$

**Output:**  $S$

```

1:  $x \leftarrow \text{Random}(1 \dots \beta^*|S|)$ 
2: for  $i = 1$  to  $x$  do
3:    $y = \text{Random}(1 \dots |S|)$ 
4:    $S'[y] \leftarrow \text{Replace}(G, S')$ 
5: end for
6:  $S_1 \leftarrow \text{select a member in EA randomly}$ 
7:  $S_2 \leftarrow \text{select a member in EA randomly}$ 
8:  $p \leftarrow \text{Random}(2 \dots (|S_1| - 1))$ 
9: for  $j = p$  to  $k$  do
10:   $S_1[i] = S_2[i]$ 
11: end for
12: return  $S$ 

```

---

#### 4. Simulation and Empirical Research.

**4.1. Experimental Design.** Our study evaluated the performance which belongs to the proposed technology with the three grid structures used in literature [15, 16, 17] (the data structures have be expressed in Table 1 and the topology of Data Set 1 can be seen in Figure 1). These three different datasets have different characteristics, divided into two types: directed graph and undirected graph. The number of nodes and the number of node boundaries are both large, providing different complex environments for algorithm validation in the following text.

Our research is based on MATLAB software for timing simulation, combined with Python framework implementation, and works on two Linux OS servers (Intel Xeon processor (34 GHZ) 64GB RAM), each has a 6-core CPU, two NVIDIA Titan X GPUs and a 100 GB RAM. Since the results of the experimental public opinion control model may be different in each run, the evaluation results are set to be the average value after 500 iterations, with the standard deviation of 1.415.

TABLE 1. Characteristics of Grid Data Set

Network Serial Number	Dataset Number	Type	Number of nodes	Number of node boundaries	Average	Node Average Path	Clustering coefficient
1	Dataset 1	Directed	2414	64959	3.19	2.12	0.429
2	Dataset 2	Undirected	2310	79610	4.18	3.41	0.120
3	Dataset 3	Directed	4285	75592	3.12	2.24	0.245

Our study compares the proposed Swarm Intelligent Optimization Algorithm for Abnormal Link Prediction (SIOA-ALP) with the benchmark algorithms mentioned in Section 3.1 and 3.2. Two precision functions, that is Mean Absolute Error (MAE) and Root Mean

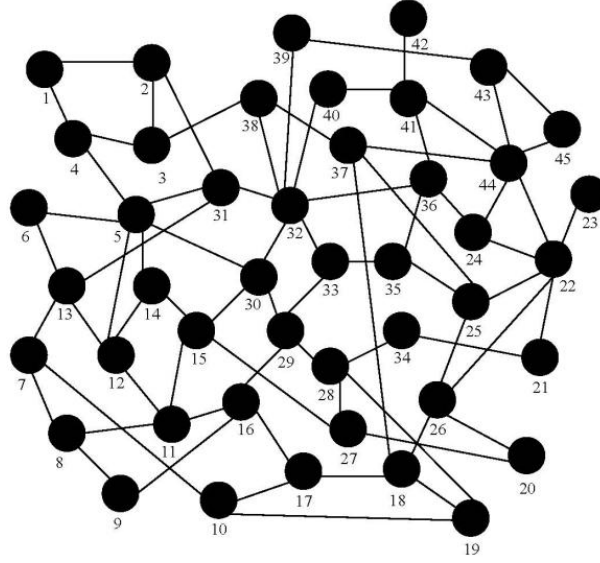


FIGURE 1. Topology grid used in the experiment.

Square Error (RMSE), which are based on the reference [30]. The specific calculation method is shown in Equation (27) and Equation (28) respectively.

$$MAE = \sqrt{\frac{1}{N} \sum_{i=1}^N |f_i - y_i|} \quad (27)$$

$$RMSE = \sqrt{\frac{1}{N} \sum_{i=1}^N (observed_i - predicted_i)^2} \quad (28)$$

Where as the problem of opinion dissemination in social networks is usually thought as a binary classification task, and shown in the matrix which is in confusion for the evaluation of binary classification tasks with two categories [11]. There are four metrics, including True Positive (TP), indicating the quantity of the links which are predicted correctly; True Negative (TN), indicating the quantity of correctly unpredicted links; False Positive (FP), indicating the quantity of incorrectly predicted links; and False Negative (FN), indicating the quantity of incorrectly unpredicted links. Based on this, the following metrics are obtained, such as True Case Rate/Recall Rate/Sensitivity. Among them, the calculation of True Positive Rate (TPR), False Positive Rate (FPR), True Negative Rate (TNR) and Precision Rate (PR) can be found in the literature [26]. And the results can be evaluated based on two metrics, namely the Area Under the Receiver Operating Characteristics curve (AUROC) [18] and the Average Precision (AP) [19]. The ROC curve describes the true case rate on the Y-axis (sensitivity) and the false positive rate (1-specificity) on the X-axis. Meanwhile, the area which is located under the ROC curve is the single point summary statistics between  $[0, 1]$ , which can be calculated following the trapezoidal rule, summing every trapezoids under the curve. The AUROC value of the link prediction method ought to be greater than 0.5, and if the AUROC value gets higher, the performance of the link prediction method can be better. The average precision can be thought as one single point summary value calculated according to different recall thresholds, and is the average precision value of the recall values when facing the interval  $[0, 1]$ . Specifically, it is shown in Equation (29). Where,  $p$  denotes the precision rate under

different recall  $r$  thresholds, and  $R$  is the set of different thresholds.

$$AP = \sum_{k=1}^R p(k)\Delta r(k) \quad (29)$$

**4.2. Experimental results.** The experimental results fully demonstrate that the SIOA-ALP algorithm proposed in this paper is superior to other general benchmark algorithms. In Table 2, we can see the area values under the curve of the SIOA-ALP anomaly link prediction swarm intelligent optimization algorithm and other benchmark methods with the grid data set. We found that the proposed SIOA-ALP swarm intelligence optimization algorithm has better experimental results. Table 3 reports the average accuracy results of SIOA-ALP anomaly link prediction swarm intelligent optimization algorithm and other benchmark social network public opinion propagation control methods. According to the results, the proposed SIOA-ALP algorithm has higher average precision in all experimental data sets. Combined with the comparison of single operation time of the algorithm shown in Table 4, the operation efficiency of the SIOA-ALP anomaly link prediction swarm intelligent optimization algorithm proposed in this research when facing the grid data set is also improved compared with other existing algorithms.

TABLE 2. Area values of different methods under the curve on each dataset

Dataset Number	CN	AA	PA	RA
Dataset 1	0.6385	0.4618	0.5713	0.6274
Dataset 2	0.4758	0.5825	0.4829	0.5028
Dataset 3	0.2104	0.5839	0.3019	0.3481
Dataset Number	LP	ERA	PIC	SIOA-ALP
Dataset 1	0.3251	0.6389	0.7095	<b>0.9127</b>
Dataset 2	0.3942	0.5692	0.4910	<b>0.9218</b>
Dataset 3	0.6484	0.4280	0.6849	<b>0.9342</b>

Note: The values shown in bold indicate good algorithm performance.

TABLE 3. Average precision values of different methods on each data set

Dataset Number	CN	AA	PA	RA
Dataset 1	0.3274	0.2618	0.2874	0.2306
Dataset 2	0.2958	0.2475	0.2503	0.3418
Dataset 3	0.1947	0.2138	0.2758	0.4537
Dataset Number	LP	ERA	PIC	SIOA-ALP
Dataset 1	0.2959	0.2419	0.4827	<b>0.6838</b>
Dataset 2	0.3859	0.4582	0.3058	<b>0.7652</b>
Dataset 3	0.3471	0.4857	0.3195	<b>0.6748</b>

Note: The values shown in bold indicate good model performance.

In conjunction with the literature [36], two precision functions are used here: Mean Absolute Error (MAE) and Root Mean Square Error (RMSE). Table 5 reports the MAE and RMSE values which belong to the proposed SIOA-ALP anomaly link prediction swarm intelligent optimization algorithm and other benchmark algorithms in different grid topologies. Higher the MAE and RMSE values show lower the precision of the predictive optimization algorithm. According to Table 5, the proposed grid optimization algorithm generally outperforms other methods, because the proposed SIOA-ALP anomaly link

TABLE 4. Comparison of single run time of algorithms

Dataset Number	CN	AA	PA	RA
Dataset 1	0.1419	0.5121	5.1410	3.2419
Dataset 2	0.6378	4.2218	6.4833	9.0412
Dataset 3	0.8124	1.0422	7.1923	5.5407
Dataset Number	LP	ERA	PIC	SIOA-ALP
Dataset 1	0.1538	0.2759	0.4634	<b>0.1324</b>
Dataset 2	0.4269	0.5846	0.6504	<b>0.1726</b>
Dataset 3	0.2435	0.4763	0.3638	<b>0.1449</b>

Note: The bold section indicates that the algorithm is relatively optimal under this parameter condition.

prediction swarm intelligent optimization algorithm has the capability of quick response and real-time adjustment and optimization of the power grid, and it can also minimize the grid loss.

TABLE 5. Comparison Results of Algorithms in Grid Topology

	Index	CN	AA	PA	RA
Actual value	MAE	0.5839	0.5374	0.5741	0.4829
	RMSE	0.6342	0.6103	0.5927	0.5840
Optimum value	MAE	0.5648	0.5829	0.5384	0.5390
	RMSE	0.7302	0.6817	0.6739	0.7028
	Index	LP	ERA	PIC	SIOA-ALP
Actual value	MAE	0.4291	0.5443	0.5738	<b>0.3204</b>
	RMSE	0.5831	0.5603	0.6023	<b>0.4210</b>
Optimum value	MAE	0.4135	0.5024	0.5381	<b>0.2804</b>
	RMSE	0.5582	0.5128	0.5429	<b>0.3452</b>

Note: The bold section indicates that the algorithm is relatively optimal under this parameter condition.

**4.3. Statistical test.** That statistical test has been performed for this study with reference to the literature [23] to report the significant differences between the proposed grid voltage optimization methods and other benchmark methods. The Friedman test [47] was used in this study to think whether there is an important difference between these grid voltage optimization methods, which is a nonparametric pairwise analysis of measures ANOVA which is repeated. The results of the Friedman test which belongs to the area under the ROC curve (AUROC value) and the average accuracy (AP value) can be seen from Table 6. The observed test values of the Friedman test for AUROC and AP,  $F_f$ , were 49.242 and 62.220 respectively, which were greater than the corresponding  $\chi^2$  values. As the confidence interval  $\alpha = 0.05$ , the degree of freedom  $D_f = 8$ , and the  $\chi^2$  value is 16.25, the null hypothesis is rejected.

As the null hypothesis has been rejected, an post-hoc test will be performed. The Friedman-Conversover post-hoc method is chosen to control the proposed optimization method, and the normal Holm is used as the adjustment method. The Friedman-Converover multiple comparison test results have expressed in Table 7. Meanwhile, the p-values are corrected for AUROC and AP values using Holm method. It can be known according to the table that the proposed grid voltage optimization method is significantly different from other baseline methods, so there are significant differences between those methods.

TABLE 6. Friedman Test Results for AUROC and AP Values

Metric	Dataset Number	CN	AA	PA	RA
AUROC	Dataset 1	0.8348	0.9604	0.9856	0.9349
	Dataset 2	0.8924	0.9340	0.9172	0.9647
	Dataset 3	0.7827	0.7818	0.8104	0.7832
AP	Dataset 1	0.0030	0.0053	0.0025	0.1937
	Dataset 2	0.0266	0.0514	0.3738	0.2291
	Dataset 3	0.2514	0.3374	0.2438	0.1081
Metric	Dataset Number	LP	ERA	PIC	SIOA-ALP
AUROC	Dataset 1	0.8035	0.7588	0.8572	0.7483
	Dataset 2	0.8464	0.8371	0.7580	0.7563
	Dataset 3	0.8938	0.8593	0.7583	0.8192
AP	Dataset 1	0.2482	0.3022	0.3922	0.6393
	Dataset 2	0.2381	0.3229	0.3185	0.6255
	Dataset 3	0.2859	0.3315	0.3846	0.6492

TABLE 7. Friedman-Convover multiple comparison test results (the control method is the proposed algorithm, and the correction method is Holm method)

Metric	CN	AA	PA	RA
AUROC value	0.0001	0.0002	0.0094	0.0013
AP value	0.0001	0.0006	0.0005	0.0008
Metric	LP	ERA	PIC	SIOA-ALP
AUROC value	0.0014	0.0043	0.0153	0.0021
AP value	0.0032	0.0058	0.0046	0.0086

**5. Conclusion.** In this research, we constructed a complex meshwork model of the power network by subspace reconstruction and availability analysis method, and designed the prediction algorithm for the grid link network, which is improved by combining the anomaly value and the improved Dijkstra algorithm, and then we used the improved bee colony algorithm to solve the model, so as to improve the high availability of the data service in the complex multi-network center environment of the grid. The algorithm model proposed in this article has multiple innovations. It not only proposes optimization schemes based on benchmark algorithms such as bee colony algorithm and so on, but also innovatively integrates some parameter optimization methods and provides innovative solutions for intelligent prediction and data service prediction of power grids. Experimental results have expressed that the Swarm Intelligent Optimization Algorithm for Abnormal Link Prediction (SIOA-ALP) has better accuracy and efficiency than other benchmark algorithms. Despite these important findings, this study has some limitations, some of which may point the way for future further research. Firstly, the uncertainty of both nodes and edges can be considered in the link prediction algorithm, which can further improve the ability of the algorithm which is proposed to resist uncertainty. Secondly, the applicability of the algorithm which is proposed can be verified in protein network, terrorist network, scientific cooperative network and multi-layer network. Finally, advanced techniques such as deep self-encoder will be used to better the precision and efficiency which belong to the link prediction algorithm.



**Acknowledgement.** This work supported by the “Key Technologies of Digital Power Grid” (Project No.: 2020YFB0906000).

## REFERENCES

- [1] J. He, K. Chen, M. Li, Y. Luo, C. Liang, and Y. Xu, “Review of protection and fault handling for a flexible dc grid,” *Protection and Control of Modern Power Systems*, vol. 5, no. 1, pp. 1–15, 2020.
- [2] M. F. Palangar, S. Mohseni, M. Mirzaie, and A. Mahmoudi, “Designing an automatic detector device to diagnose insulator state on overhead distribution lines,” *IEEE Transactions on Industrial Informatics*, vol. 18, no. 2, pp. 1072–1082, 2021.
- [3] M. J. E. Alam, K. M. Muttaqi, and D. Sutanto, “A multi-mode control strategy for var support by solar pv inverters in distribution networks,” *IEEE Transactions on Power Systems*, vol. 30, no. 3, pp. 1316–1326, 2014.
- [4] M.-F. Qu, N. Chen, and Y.-Q. Liu, “Grid-connected control method for new energy inverter based on single chip micoyo,” *International Journal of Critical Infrastructures*, vol. 17, no. 3, pp. 204–215, 2021.
- [5] M. Li, H. Xiao, and M. Cheng, “An adaptive strategy based on repetitive predictive control for improving adaptability of lcl-type grid-connected inverters under weak grid,” *IEEE Transactions on Power Electronics*, vol. 37, no. 3, pp. 2562–2572, 2021.
- [6] J. Liu and M. Molinas, “Impact of digital time delay on the stable grid-hosting capacity of large-scale centralised pv plant,” *IET Renewable Power Generation*, vol. 15, no. 7, pp. 1422–1435, 2021.
- [7] A. Rajaram and K. Sathiyaraj, “An improved optimization technique for energy harvesting system with grid connected power for green house management,” *Journal of Electrical Engineering & Technology*, vol. 17, no. 5, pp. 2937–2949, 2022.
- [8] L. Zhou, M. Jahnes, M. Eull, W. Wang, and M. Preindl, “Control design of a 99efficiency transformerless ev charger providing standardized grid services,” *IEEE Transactions on Power Electronics*, no. 37-4, pp. 4022–4038, 2022.
- [9] M. B. Delghavi and S. Pashaei Choboghloo, “Voltage sag mitigation in der-connected distribution networks by statcom,” *Electric Power Components and Systems*, vol. 48, no. 19-20, pp. 2156–2167, 2021.
- [10] Z. Xie, E. Dong, J. Li, D. Kong, and N. Wu, “Potential links by neighbor communities,” *Physica A: Statistical Mechanics and its Applications*, vol. 406, pp. 244–252, 2014.
- [11] R. Dharavath and N. S. Arora, “Spark’s graphx-based link prediction for social communication using triangle counting,” *Social Network Analysis and Mining*, vol. 9, pp. 1–12, 2019.
- [12] L. Srivastava and H. Singh, “Hybrid multi-swarm particle swarm optimisation based multi-objective reactive power dispatch,” *IET Generation, Transmission & Distribution*, vol. 9, no. 8, pp. 727–739, 2015.
- [13] S. Samanta, J. P. Mishra, and B. K. Roy, “Implementation of a virtual inertia control for inertia enhancement of a dc microgrid under both grid connected and isolated operation,” *Computers & Electrical Engineering*, vol. 76, pp. 283–298, 2019.
- [14] D. Xu and H. Cen, “A hybrid energy storage strategy based on multivariable fuzzy coordinated control of photovoltaic grid-connected power fluctuations,” *IET Renewable Power Generation*, vol. 15, no. 8, pp. 1826–1835, 2021.
- [15] S. N. Salih and P. Chen, “On coordinated control of oltc and reactive power compensation for voltage regulation in distribution systems with wind power,” *IEEE Transactions on Power Systems*, vol. 31, no. 5, pp. 4026–4035, 2015.
- [16] S. Gao, L. Zhou, X. Wang, and H. Chen, “Link prediction via local structural information in complex networks,” in *2017 13th International Conference on Natural Computation, Fuzzy Systems and Knowledge Discovery (ICNC-FSKD)*. IEEE, 2017, pp. 2247–2253.
- [17] T. Pan, S. Mishra, L. N. Nguyen, G. Lee, J. Kang, J. Seo, and M. T. Thai, “Threat from being social: Vulnerability analysis of social network coupled smart grid,” *IEEE Access*, vol. 5, pp. 16 774–16 783, 2017.
- [18] G. C. Kryonidis, N. V. Theologou, A. I. Chrysochos, C. S. Demoulias, and G. K. Papagiannis, “An enhanced decentralized voltage regulation scheme for the reduction of tap changes in hv/mv transformers under high dg penetration,” in *2016 IEEE PES Innovative Smart Grid Technologies Conference Europe (ISGT-Europe)*. IEEE, 2016, pp. 1–6.

- [19] W. Sheng, K.-Y. Liu, S. Cheng, X. Meng, and W. Dai, "A trust region sqp method for coordinated voltage control in smart distribution grid," *IEEE Transactions on Smart Grid*, vol. 7, no. 1, pp. 381–391, 2015.
- [20] Y. Tang, K. Dvijotham, and S. Low, "Real-time optimal power flow," *IEEE Transactions on Smart Grid*, vol. 8, no. 6, pp. 2963–2973, 2017.
- [21] L. Shang, X. Dong, C. Liu, and W. He, "Modelling and analysis of electromagnetic time scale voltage variation affected by power electronic interfaced voltage regulatory devices," *IEEE Transactions on Power Systems*, vol. 37, no. 2, pp. 1102–1112, 2021.
- [22] J. F. Franco, L. F. Ochoa, and R. Romero, "Ac opf for smart distribution networks: An efficient and robust quadratic approach," *IEEE Transactions on Smart Grid*, vol. 9, no. 5, pp. 4613–4623, 2017.
- [23] A. M. Shaheen, R. A. El-Sehiemy, and S. M. Farrag, "Solving multi-objective optimal power flow problem via forced initialised differential evolution algorithm," *IET Generation, Transmission & Distribution*, vol. 10, no. 7, pp. 1634–1647, 2016.
- [24] X. Zheng, W. Pan, X. Liu, and Y. He, "Primary double winding coupling dc transformer for dc micro-grid applications," *Journal of Electrical Engineering & Technology*, vol. 17, no. 3, pp. 1679–1691, 2022.
- [25] P. Panigrahi and S. Maity, "Structural vulnerability analysis in small-world power grid networks based on weighted topological model," *International Transactions on Electrical Energy Systems*, vol. 30, no. 7, pp. 1–18, 2020.
- [26] L. Zhang, W. Tang, J. Liang, P. Cong, and Y. Cai, "Coordinated day-ahead reactive power dispatch in distribution network based on real power forecast errors," *IEEE Transactions on Power Systems*, vol. 31, no. 3, pp. 2472–2480, 2015.
- [27] S. Haghani and M. R. Keyvanpour, "A systemic analysis of link prediction in social network," *Artificial Intelligence Review*, vol. 52, pp. 1961–1995, 2019.
- [28] R. Mahapatra, S. Samanta, M. Pal, and Q. Xin, "Rsm index: a new way of link prediction in social networks," *Journal of Intelligent & Fuzzy Systems*, vol. 37, no. 2, pp. 2137–2151, 2019.
- [29] A. Bektache and B. Boukhezzar, "Nonlinear predictive control of a dfig-based wind turbine for power capture optimization," *International journal of electrical power & Energy systems*, vol. 101, pp. 92–102, 2018.
- [30] H. G. Yeh, D. F. Gayme, and S. H. Low, "Adaptive var control for distribution circuits with photovoltaic generators," *IEEE Transactions on Power Systems*, vol. 27, no. 3, pp. 1656–1663, 2012.
- [31] L. Lü and T. Zhou, "Link prediction in complex networks: A survey," *Physica A: Statistical Mechanics and Its Applications*, vol. 390, no. 6, pp. 1150–1170, 2011.
- [32] Z. Shuai, D. He, Z. Xiong, Z. Lei, and Z. J. Shen, "Comparative study of short-circuit fault characteristics for vsc-based dc distribution networks with different distributed generators," *IEEE Journal of Emerging and Selected Topics in Power Electronics*, vol. 7, no. 1, pp. 528–540, 2018.
- [33] C.-G. Yun, S. Baek, H. Bu, Y. Cho, J.-H. Park, and M.-Y. Kim, "Simple current control without grid voltage sensor for traction solid-state transformer," *Journal of Power Electronics*, vol. 21, pp. 703–712, 2021.
- [34] S. Sankararaman, "Complex network analysis of the thermal lens signal: a markov model approach," *Applied Optics*, vol. 60, no. 22, pp. 6409–6413, 2021.
- [35] C. Lei and J. Ruan, "A novel link prediction algorithm for reconstructing protein–protein interaction networks by topological similarity," *Bioinformatics*, vol. 29, no. 3, pp. 355–364, 2013.
- [36] J. Peng, G. Lu, and X. Shang, "A survey of network representation learning methods for link prediction in biological network," *Current Pharmaceutical Design*, vol. 26, no. 26, pp. 3076–3084, 2020.
- [37] R. Yan, Y. Li, D. Li, W. Wu, and Y. Wang, "Ssdbs: the stretch shrink distance based algorithm for link prediction in social networks," *Frontiers of Computer Science*, vol. 15, pp. 1–8, 2021.
- [38] J.-H. Choi and B.-J. Choi, "Indoor moving and implementation of a mobile robot using hall sensor and dijkstra algorithm," *IEMEK Journal of Embedded Systems and Applications*, vol. 14, no. 3, pp. 151–156, 2019.
- [39] S.-K. Zhang, C.-T. Li, and S.-D. Lin, "A joint optimization framework for better community detection based on link prediction in social networks," *Knowledge and Information Systems*, vol. 62, no. 1, pp. 4277–4296, 2020.
- [40] S. M. Abd Elazim and E. S. Ali, "Optimal network restructure via improved whale optimization approach," *International Journal of Communication Systems*, vol. 34, no. 1, p. e4617, 2021.

- [41] E. Nasiri, K. Berahmand, M. Rostami, and M. Dabiri, "A novel link prediction algorithm for protein-protein interaction networks by attributed graph embedding," *Computers in Biology and Medicine*, vol. 137, p. 104772, 2021.
- [42] T. Derr, Z. Wang, J. Dacon, and J. Tang, "Link and interaction polarity predictions in signed networks," *Social Network Analysis and Mining*, vol. 10, pp. 1–14, 2020.
- [43] H. Yuliansyah, Z. A. Othman, and A. A. Bakar, "Extending adamic adar for cold-start problem in link prediction based on network metrics," *International Journal of Advances in Intelligent Informatics*, vol. 8, no. 3, pp. 271–284, 2022.
- [44] M. A. Hasan and M. J. Zaki, "A survey of link prediction in social networks," *Social Network Data Analytics*, pp. 243–275, 2011.
- [45] X. Tao, B. Xiong, and Q. An, "Dea-based centralized resource allocation with network flows," *International Transactions in Operational Research*, vol. 28, no. 2, pp. 926–958, 2021.
- [46] P. Wang, B. Xu, Y. Wu, and X. Zhou, "Link prediction in social networks: the state-of-the-art," *arXiv preprint arXiv:1411.5118*, 2014.
- [47] F. Aghabozorgi and M. R. Khayyambashi, "A new similarity measure for link prediction based on local structures in social networks," *Physica A: Statistical Mechanics and its Applications*, vol. 501, pp. 12–23, 2018.
- [48] X. Li, S. Liu, H. Chen, and K. Wang, "A potential information capacity index for link prediction of complex networks based on the cannikin law," *Entropy*, vol. 21, no. 9, p. 863, 2019.
- [49] F. Aghabozorgi and M. Reza Khayyambashi, "A new study of using temporality and weights to improve similarity measures for link prediction of social networks," *Journal of Intelligent & Fuzzy Systems*, vol. 34, no. 4, pp. 2667–2678, 2018.
- [50] X.-K. Xu, K.-K. Shang, and J. Xiao, "Quantifying the effect of community structures for link prediction by constructing null models," *IEEE Access*, vol. 8, pp. 89 269–89 280, 2020.
- [51] M. Liu, Y. Ma, Z. Cao, and X. Qi, "Ecp-rank: a novel vital node identifying mechanism combining pagerank with link prediction index," *Physica A: Statistical Mechanics and Its Applications*, vol. 512, pp. 1183–1191, 2018.
- [52] R. Huang, L. Ma, G. Zhai, J. He, X. Chu, and H. Yan, "Resilient routing mechanism for wireless sensor networks with deep learning link reliability prediction," *IEEE Access*, vol. 8, pp. 64 857–64 872, 2020.
- [53] Y. Su, X. Meng, Z. Yu, and Q. Kang, "Cognitive virtual network topology reconfiguration method based on traffic prediction and link importance," *IEEE Access*, vol. 7, pp. 138 915–138 926, 2019.
- [54] J. C. Valverde-Rebaza and A. de Andrade Lopes, "Link prediction in complex networks based on cluster information," pp. 92–101, 2012.
- [55] R. Barham, A. Sharieh, and A. Sleit, "Multi-moth flame optimization for solving the link prediction problem in complex networks," *Evolutionary Intelligence*, vol. 12, no. 4, pp. 563–591, 2019.
- [56] M. A. Naoui, B. Lejdel, M. Ayad, R. Belkeiri, and A. S. Khaouazm, "Integrating deep learning, social networks, and big data for healthcare system," *Bio-Algorithms and Med-Systems*, vol. 16, no. 1, p. 20190043, 2020.
- [57] S. Mallek, I. Boukhris, Z. Elouedi, and E. Lefevre, "The link prediction problem under a belief function framework," in *2015 IEEE 27th International Conference on Tools with Artificial Intelligence (ICTAI)*. IEEE, 2015, pp. 1013–1020.
- [58] J. Yang, L. Yang, and P. Zhang, "A new link prediction algorithm based on local links," in *Web-Age Information Management: WAIM 2015 International Workshops: HENA, HRSUNE, Qingdao, China, June 8-10, 2015, Revised Selected Papers*. Springer, 2015, pp. 16–28.
- [59] R. Korkmaz Tan and Ş. Bora, "Adaptive modified artificial bee colony algorithms (amabc) for optimization of complex systems," *Turkish Journal of Electrical Engineering and Computer Sciences*, vol. 28, no. 5, pp. 2602–2629, 2020.
- [60] S. Sharma, S. Kumar, and K. Sharma, "Improved gbest artificial bee colony algorithm for the constraints optimization problems," *Evolutionary Intelligence*, vol. 14, pp. 1271–1277, 2021.
- [61] S. Banerjee, M. Jenamani, and D. K. Pratihari, "Combim: A community-based solution approach for the budgeted influence maximization problem," *Expert Systems with Applications*, vol. 125, pp. 1–13, 2019.
- [62] W.-H. Tan and J. Mohamad-Saleh, "Mo-nfsa for solving unconstrained multi-objective optimization problems," *Engineering with Computers*, vol. 38, no. 3, pp. 2527–2548, 2022.
- [63] J. Valverde-Rebaza and A. de Andrade Lopes, "Exploiting behaviors of communities of twitter users for link prediction," *Social Network Analysis and Mining*, vol. 3, pp. 1063–1074, 2013.

- [64] T.-Y. Wu, Y.-Q. Lee, C.-M. Chen, Y. Tian, and N. A. Al-Nabhan, "An enhanced pairing-based authentication scheme for smart grid communications," *Journal of Ambient Intelligence and Humanized Computing*, pp. 1–13, 2021.
- [65] T.-Y. Wu, H. Li, and S.-C. Chu, "Cppe: An improved phasmatodea population evolution algorithm with chaotic maps," *Mathematics*, vol. 11, no. 9, p. 1977, 2023.
- [66] C.-M. Chen, S. Lv, J. Ning, and J. M.-T. Wu, "A genetic algorithm for the waitable time-varying multi-depot green vehicle routing problem," *Symmetry*, vol. 15, no. 1, p. 124, 2023.
- [67] A. L. H. P. Shaik, M. K. Manoharan, A. K. Pani, R. R. Avala, and C.-M. Chen, "Gaussian mutation–spider monkey optimization (gm-smo) model for remote sensing scene classification," *Remote Sensing*, vol. 14, no. 24, p. 6279, 2022.